

LITERATURE DISCREPANCY: WHAT IS THE MOLAR ABSORPTIVITY OF ABTS?

Tanor Morinaka* and Todd P. Silverstein†

Chemistry Department, Willamette University, Salem, OR 97301

Abstract

In 1975 Childs and Bardsley first described the now widely-used redox chromophore ABTS [2,2'-azino-bis(3-ethylbenzthiazoline-6-sulfonate)], reporting that the molar absorptivity of the prominent visible region peak at 414 nm for the oxidized ABTS^{•+} radical was 36 mM⁻¹cm⁻¹. Since then, many authors have reported ϵ_{414} values in the 31 – 37 mM⁻¹cm⁻¹ range, but many others have reported $\epsilon_{414} = 26 - 28$ mM⁻¹cm⁻¹. Here we carefully characterize the kinetics of ABTS: oxidation, first to ABTS^{•+}, and then to ABTS²⁺. After accounting for the second oxidation step, we find ϵ_{414} of ABTS^{•+} to be 26.0 ± 0.4 mM⁻¹cm⁻¹ in phosphate buffer at pH 6. We discuss possible reasons for the discrepancy between the two molar absorptivity values.

†Corresponding author:tsilvers@willamette.edu

*Undergraduate research co-author

Keywords: ABTS; spectrophotometry; UV-vis absorbance; oxidation-reduction; redox titration; chromophore; oxidants; free radical-

Submitted: September 7, 2022

Accepted: September 19, 2022

Published: October 21, 2022

Introduction

The redox chromophore ABTS [2,2'-azino-bis(3-ethylbenzthiazoline-6-sulfonate)] is widely used in the spectrophotometric analysis of oxidants¹, especially free radicals,²⁻⁴ peroxides,⁵⁻¹⁵ transition metal complexes,¹⁶⁻²⁰ and halogens^{16,21}. Lately, ABTS has also been used to measure antioxidant activity in natural products and biological samples.²²⁻²⁸

Reduced ABTS, which is colorless ($\epsilon_{340} = 36$ mM⁻¹cm⁻¹, ref.5), can lose an electron to form the amine radical ABTS^{•+} (Figure S1, Appendix). This blue-green compound has three visible absorbance peaks, with the most prominent at ≈ 415 nm. The peak around 730 nm is less intense, but it is sometimes used because interfering absorbances from other compounds at this wavelength are rare.

In their initial paper introducing the use of ABTS to detect H₂O₂, Childs and Bardsley reported a molar absorptivity of 36 mM⁻¹cm⁻¹ for both the reduced ABTS: (ϵ_{340}) and the oxidized ABTS^{•+} radical (ϵ_{414}).⁵ Their spectrophotometric redox titration curve (Figure 1) supported the former value: $\epsilon_{340}(\text{ABTS}) = 1.8$ ($A_{340})/0.050$ mM/1.00 cm = 36 mM⁻¹cm⁻¹; however, the molar absorptivity of the oxidized ABTS^{•+} was clearly significantly lower. From their spectra, one can calculate $\epsilon_{414}(\text{ABTS}^{\bullet+}) = 1.125$ ($A_{414})/0.050$ mM/1.00 cm = 22.5 mM⁻¹cm⁻¹. Finally, correcting for the 12% of ABTS: that remained unoxidized after the last addition of H₂O₂, as judged by the remaining small peak at 340 nm, we get $\epsilon_{414}(\text{ABTS}) = 25.6$ mM⁻¹cm⁻¹. In agreement with this, Maruthamuthu et al. reported $\epsilon_{417}(\text{ABTS}^{\bullet+}) = 27$ mM⁻¹cm⁻¹.¹⁶ However, Scott et al. criticized this latter value and reported $\epsilon_{417}(\text{ABTS}^{\bullet+}) = 34.7$ mM⁻¹cm⁻¹ at pH 0, in agreement with Childs and Bardsley's value.¹⁷ On the other hand, the spectrophotometric redox titration of ABTS: with Ce⁴⁺ published by Scott et al. clearly showed the final ABTS^{•+} peak at 417 nm to be 20.5% lower than the initial ABTS: peak at 340 nm; thus, their measured value of $\epsilon_{417}(\text{ABTS}^{\bullet+})$ should actually be 27.6 mM⁻¹cm⁻¹. This latter value agrees with the value of Maruthamuthu et al. (criticized by Scott et al.) and the value of Childs & Bardsley calculated from their own spectrophotometric redox titration (Figure 1).

Over the years, the molar absorptivities for ABTS^{•+} reported by Childs & Bardsley and Scott et al. (36 and 34.7 mM⁻¹cm⁻¹, respectively) were cited and employed by many researchers.^{2,3,4,9,12,24} Interestingly, however, researchers who independently determined the molar absorptivity of ABTS^{•+} reported values that clustered in the two distinct regions reported by Childs/Scott vs. Maruthamuthu et al. (Table 1).

Of the 17 reported ABTS^{•+} molar absorptivities in Table 1, 12 were “high” as reported by Childs/Scott: average = 33.7 ± 1.7 mM⁻¹cm⁻¹ (range: 31 – 37), while 5 were “low” (cf. Maruthamuthu et al.¹⁶): average = 27.1 ± 1.0 mM⁻¹cm⁻¹ (range: 26 – 28). Note that the difference between these two sets of values is greater than two standard deviations. The “high” values were measured mostly at pH -0.5 to 4.4, however, three were measured at pH 6 – 8. The “low” values were measured mostly at pH 4.5 – 6.5, but one was measured at pH 0. At first glance, one might be tempted to conclude, as did Pinkernell et al.^{10,21} and Wang and Reckhow¹, that “higher pH results in lower apparent values of ϵ .” However, this seems unlikely for two reasons. First, 3 of the 12 “high” values (25%) were measured at high pH, while 1 of the 5 “low” values

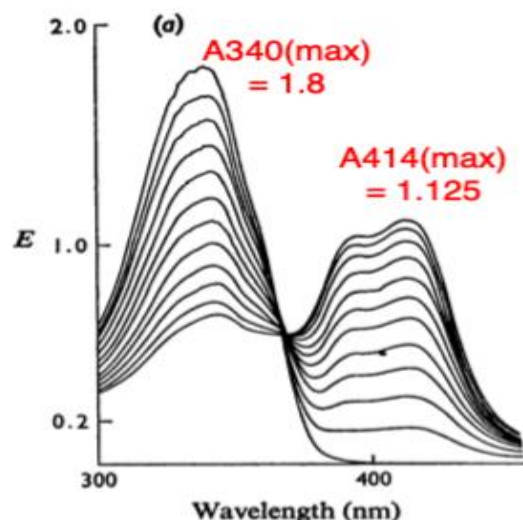


Figure 1. Spectrophotometric redox titration of ABTS with H₂O₂ in phosphate buffer, pH 6.0. Adapted from ref.5.

(20%) was measured at low pH. Based on the entire sample set of all literature values, any dependence on pH seems to be statistically insignificant: Averaging all molar absorptivities obtained at pH < 5, we get $32 \pm 3 \text{ mM}^{-1}\text{cm}^{-1}$, and for those at pH ≥ 6 , $31 \pm 5 \text{ mM}^{-1}\text{cm}^{-1}$. The difference of only $1 \text{ mM}^{-1}\text{cm}^{-1}$ is clearly not statistically significant, with $P = 0.5$. Alternatively, fitting all of the reported values in Table 1 to the pH-dependence expected for an acid-base titration (Fig. S2, Appendix), the R^2 value for the resulting fit is low (0.1), the Chi-square value is high (174), and the fitted $\text{p}K_a$ (3.6 ± 3.2) has an uncertainty nearly as large as its value.

Furthermore, ABTS: has only a single titratable group (the azino $-\text{NH}^+=$ group)⁷ whose $\text{p}K_a$ has been found¹⁷ to be 2.1, while the oxidized ABTS $^{\cdot+}$ radical has no titratable group at all ($\text{p}K_a < 0$).¹⁷ For pH > 3, ABTS: and ABTS $^{\cdot+}$ will both be deprotonated, and their physical characteristics should not change with pH. This in fact matches results reported for the pH range 3 to 10.5.^{7,29} Thus, the contention that the ABTS $^{\cdot+}$ molar absorptivity is pH-dependent is not supported by experimental evidence.

Noting that in the narrow range $6.0 < \text{pH} < 7.5$, ABTS $^{\cdot+}$ molar absorptivities of both 27 and $35 \text{ mM}^{-1}\text{cm}^{-1}$ were reported, we set out to carefully measure the value at pH 6.0. ABTS: can be oxidized by strong oxidizing agents (e.g., permanganate, persulfate, Cr(VI)), but in the absence of catalysts, the reaction can take hours.²⁴ If peroxide is the oxidant, then the enzyme peroxidase effectively catalyzes ABTS: oxidation. We have characterized the double-exponential kinetics of peroxidase-catalyzed ABTS: oxidation to ABTS $^{\cdot+}$, and its subsequent oxidation to ABTS $^{2+}$. By separating these two processes, we have created careful standard curves showing that ϵ_{414} for ABTS $^{\cdot+} = 26.0 \pm 0.4 \text{ mM}^{-1}\text{cm}^{-1}$.

Experimental Methods

All reagents were purchased at maximum purity from Sigma-Aldrich; stock solutions were kept on ice. Spectrophotometric measurements were made with a Varian Cary-3 UV-Vis spectrophotometer at room temperature, unless otherwise specified. In order to make the ABTS: calibration curve for absorbances at 340 nm, sample solutions were placed in quartz cuvettes containing a

Table 1. Reported literature values of the molar absorptivity of ABTS.

pH	λ_{max} (nm)	$\epsilon_{\lambda_{\text{max}}}$ ($\text{mM}^{-1}\text{cm}^{-1}$)	Reference	comments
-0.5	415	36.9 ± 0.1	Fan ¹⁹	
0	417	34.7	Scott ¹⁷	
0	417	27.6	Scott ¹⁷	Calculated*
2	405	31.6 ± 0.2	Pinkernell ¹⁰	
2	415	33.0 ± 0.2	Pinkernell ¹⁰	From Fig. 1
2	415	33.6 ± 0.5	Wang ¹	
2.1	415	33.4 ± 0.4	Wang ¹	
4.2	415	33.0 ± 0.1	Lee ¹⁸	
4.3	414	31.1 ± 0.2	Arnao ⁸	
4.5	414	26.7	Arnao ²²	From Fig. 1
4.4	412	32.4	Shindler ⁶	
6.0	414	36	Childs ⁵	
6.0	414	25.6	Childs ⁵	Calculated*
6.0	417	27	Maruthamuthu ¹⁶	
6.5	405	28.5 ± 1.0	Pinkernell ²¹	
7.5	414	33	Cano ²³	From Fig. 1
8	420	35.7	Van Hellemond ¹²	?**

* calculated from the A_{417}/A_{340} peak height ratio

** value reported at pH 8, 420 nm, but cited Childs & Bardsley (at pH 6, 414 nm; ref.⁵)

final volume of 3.0 mL; sample cuvettes were blanked with a reference cuvette containing deionized water. For all ABTS: oxidation reactions, semi-micro plastic cuvettes contained a final volume of 1.0 mL. The sample cuvette contained final concentrations of 0.5 μM horseradish peroxidase, 0.1 M phosphate buffer (pH 6.0), 0 – 100 μM ABTS:, and $[\text{H}_2\text{O}_2] = 4 \cdot [\text{ABTS:}]$; the reference cuvette contained everything except the enzyme. Nonlinear regression of absorbance kinetic traces was performed with Kaleidagraph software.

Results

We determined the molar absorptivity of the reduced ABTS: chromophore to be $\epsilon_{340} = 39.4 \pm 0.3 \text{ mM}^{-1}\text{cm}^{-1}$ (Figure S3, Appendix), in reasonably good agreement with the values determined by Childs and Bardsley and Scott *et al.* (36 and $36.6 \text{ mM}^{-1}\text{cm}^{-1}$, respectively).^{5,17}

For the peroxidase-catalyzed oxidation of ABTS: by H_2O_2 , we were able to fit the fast rise in A_{414} due to ABTS $^{\cdot+}$ formation, followed by the slow fall in A_{414} due to further oxidation of ABTS $^{\cdot+}$ to ABTS $^{2+}$, to double-exponential kinetics (Equation 1):

$$\text{Equation 1: } A_t = A_{\text{final}} + \Delta A_{\text{fast}} \cdot e^{-k_{\text{fast}} \cdot t} + \Delta A_{\text{slow}} \cdot e^{-k_{\text{slow}} \cdot t}$$

where k_i is a first-order rate constant (in s^{-1}), ΔA_i is the amplitude of the first-order process (negative for rising absorbance, and positive for falling absorbance), and A_{final} is the asymptotic absorbance as $t \rightarrow \text{infinity}$. It can be shown that the initial absorbance, $A_0 = A_{\text{final}} + \Delta A_{\text{fast}} + \Delta A_{\text{slow}}$; also, the absorbance due to complete oxidation of the initial ABTS: to ABTS $^{\cdot+}$, without any subsequent loss of ABTS $^{\cdot+}$ from further oxidation = $A_{\text{max}} = A_0 + |\Delta A_{\text{fast}}| = A_{\text{final}} + \Delta A_{\text{slow}}$. Data for the oxidation of 25 μM ABTS: in the presence of 1 mM H_2O_2 are shown in Figure 2. It is clear that the fit of Equation 1 (red curve) to the measured absorbances (blue points) is excellent. The residuals from this fit are plotted in Figure S4 in the Appendix.

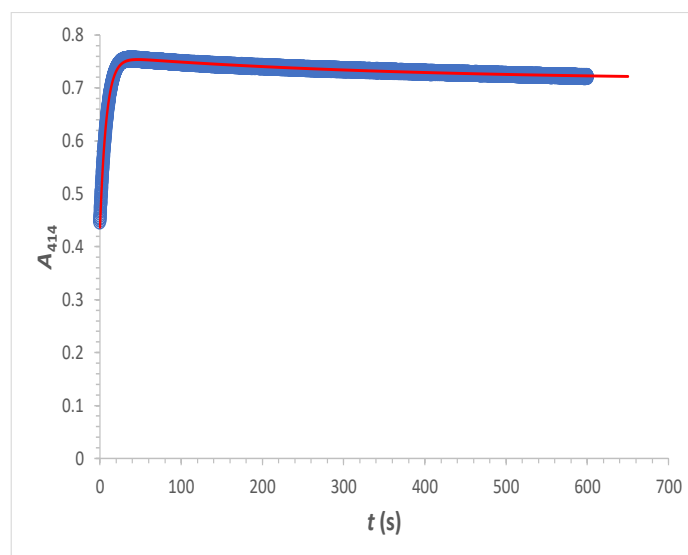


Figure 2. Peroxidase-catalyzed oxidation of 25 μM ABTS by 1 mM H_2O_2 (40-fold excess). Data (blue points) are fit to Equation 1 (red curve). The solution contained 0.5 μM horseradish peroxidase, and 0.1 M phosphate buffer, pH 6.0. Fitted parameters from nonlinear regression: $A_{\text{final}} = 0.71460 \pm 0.00017$; $\Delta A_{\text{fast}} = -0.32562 \pm 0.00027$; $k_{\text{fast}} = 7.579 \pm 0.011 \text{ min}^{-1}$; $\Delta A_{\text{slow}} = 0.04561 \pm 0.00013$; $k_{\text{slow}} = 0.1716 \pm 0.0015 \text{ min}^{-1}$; $R^2 = 0.9976$.

The average first order rate constant for ABTS: oxidation to $\text{ABTS}^{\cdot+}$ was $7.4 \pm 2.1 \text{ min}^{-1}$ (range: 4 – 11 min^{-1}). Included in this average value were reactions run with $[\text{ABTS:}] = 10\text{--}100 \mu\text{M}$, and $[\text{H}_2\text{O}_2] = 0.01\text{--}500 \text{ mM}$. As expected, A_0 , ΔA_{fast} , A_{final} , and A_{max} ($= A_{\text{final}} + \Delta A_{\text{slow}}$) were all linearly proportional to the initial concentration of ABTS:. Because A_{max} represents the absorbance due to complete oxidation of the initial ABTS: to $\text{ABTS}^{\cdot+}$ without any further oxidation, plotting A_{max} vs. initial $[\text{ABTS:}]$ yielded an accurate calibration curve and molar absorptivity for the radical $\text{ABTS}^{\cdot+}$.

In addition, because k_{slow} was generally well over 10-fold slower than k_{fast} (range: 9-fold to 230-fold), absorbances at $t < 40 \text{ s}$ represented almost exclusively the first oxidation step and could be successfully fit to a single exponential (Equation 2) indicative of the rise in $[\text{ABTS}^{\cdot+}]$:

$$\text{Equation 2: } A_t = A_0 + \Delta A_{\text{fast}} \cdot (1 - e^{-k_{\text{fast}}t})$$

The asymptotic maximum absorbance as $t \rightarrow \text{infinity} = A_{\text{max}} = A_0 + \Delta A_{\text{fast}}$, and this is linearly proportional to the maximum $[\text{ABTS}^{\cdot+}]$, which in turn equals the initial concentration of reduced ABTS:. Thus the slope of the calibration curve plotting $A_{414,\text{max}}$ vs. the initial $[\text{ABTS:}]$ would also give $\epsilon_{414}(\text{ABTS}^{\cdot+})$, the molar absorptivity of the $\text{ABTS}^{\cdot+}$ radical. From both types of calibration curves, we determined $\epsilon_{414}(\text{ABTS}^{\cdot+}) = 26.0 \pm 0.4 \text{ mM}^{-1}\text{cm}^{-1}$ (Figure 3).

Discussion

$\text{ABTS}^{\cdot+}$ molar absorptivities reported in the literature have fallen into two ranges: low ($26 - 28 \text{ mM}^{-1}\text{cm}^{-1}$) and high ($31 - 37 \text{ mM}^{-1}\text{cm}^{-1}$). A few possible explanations can be discounted: Our low value could not be due to contaminants in the stock ABTS:, because our molar absorptivity of the reduced ABTS: matched that reported by Childs and Bardsley and by Scott et al.. Alternatively, Pinkernell et al.^{10,21} and Wang and Reckhow¹ suggested that the differences were due to pH, but as we discussed in the Introduction, these pH-related differences were not statistically significant.

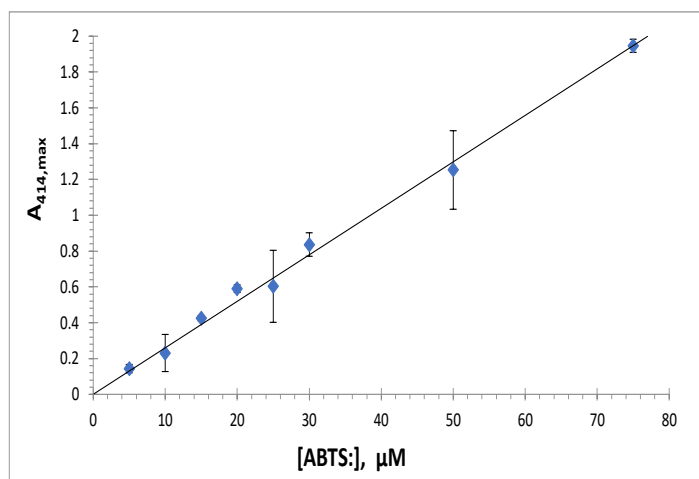


Figure 3 $\text{ABTS}^{\cdot+}$ standard curve. Solution contained $0.5 \mu\text{M}$ horseradish peroxidase, 0.1 M phosphate buffer, $\text{pH } 6.0$, and $[\text{H}_2\text{O}_2] = 4 \cdot [\text{ABTS:}]$. Triplicate samples were run at each $[\text{ABTS:}]$; error bars = 1 standard deviation. The y-intercept was statistically insignificant (0.02 ± 0.03 , $P = 0.5$), so the fit was forced through the origin: slope = $26.0 \pm 0.4 \text{ mM}^{-1}$, $R^2 = 0.998$.

The explanations that remain are calculation error and matrix effects. We believe that both of these have cropped up in the literature. The fact that both Childs & Bardsley⁵ and Scott et al.¹⁷ reported high values (36 and $34.7 \text{ mM}^{-1}\text{cm}^{-1}$, respectively), but calculations using their spectrophotometric redox titration curves yielded low values (25.6 and $27.6 \text{ mM}^{-1}\text{cm}^{-1}$, respectively), suggests a calculation error. Similarly, Arnao et al.⁸ reported a high value ($31.1 \text{ mM}^{-1}\text{cm}^{-1}$), but a calculation using their absorbance spectra (Fig. 1 in ref. ²²) yielded a low value ($26.7 \text{ mM}^{-1}\text{cm}^{-1}$); both of these Arnao et al. experiments were done in the same buffer at the same pH.

On the other hand, Pinkernell et al.¹⁰ reported a high value ($33 \text{ mM}^{-1}\text{cm}^{-1}$) at $\text{pH } 2$ in tap water acidified with acetic acid, and a low value ($28.5 \text{ mM}^{-1}\text{cm}^{-1}$) at $\text{pH } 6.5$ in phosphate buffer.²¹ It seems possible that in this case, and perhaps others, matrix effects in different buffers could account for the discrepancy.¹ This certainly bears further exploration. What we can say now with good confidence is that the molar absorptivity of $\text{ABTS}^{\cdot+}$ in phosphate buffer at $\text{pH } 6$ lies in the low range, between 26 and $28 \text{ mM}^{-1}\text{cm}^{-1}$. Furthermore, we recommend that researchers who plan to measure oxidant concentration using the molar absorptivity of $\text{ABTS}^{\cdot+}$, carefully determine its value in the appropriate solution matrix rather than rely on a particular literature value.

Acknowledgments

All of the data in this paper (and some of the text) were adapted from Tanor Morinaka's senior thesis [2013, Chemistry Department, Willamette University], done in partial fulfillment of his requirements for graduation.

References

1. Wang, T.; Reckhow, D. A. *Ozone: Sci. Engin.*, **2016**, *38*, 373–381.
2. Wolfenden, B. S.; Willson, R. L. *J. Chem. Soc., Farad. Trans. II: Molec. Chem. Phys.*, **1982**, 805–812.
3. Forni, L. G.; Mora-Arellano, V. O.; Packer, J. E.; Willson, R. L. *J. Chem. Soc., Farad. Trans. II: Molec. Chem. Phys.*, **1986**, 1–6.
4. Koleva, I. I.; Niederländer, H. A.; van Beek, T. A. *Anal. Chem.*, **2001**, *73*, 3373–3381.
5. Childs, R. E.; Bardsley, W. G. *Biochem. J.*, **1975**, *145*, 93–103.
6. Shindler, J. S.; Childs, R. E.; Bardsley, W. G. *Eur. J. Biochem.*, **1976**, *65*, 325–331.
7. Venkatasubramanian, L.; Maruthamuthu, P. *Int. J. Chem. Kin.*, **1989**, *21*, 399–421.
8. Arnao, M. B.; Acosta, M.; Del Rio, J. A.; Garcia-Canovas, F. *Biochim. Biophys. Acta - Prot. Struct. Molec. Enzymol.*, **1990**, *1038*, 85–89.
9. Pruitt, K. M.; Kamau, D. N.; Miller, K.; Månsson-Rahemtulla, B.; Rahemtulla, F. *Anal. Biochem.*, **1990**, *191*, 278–286.
10. Pinkernell, U.; Lüke, H.-J.; Karst, U. *Analyst*, **1997**, *122*, 567–571.

¹Note that Childs and Bardsley⁵ used essentially the same phosphate buffer ($\text{pH } 6$) as Pinkernell et al.. Although Childs and Bardsley reported a high value for $\epsilon_{414}(\text{ABTS}^{\cdot+})$, as recounted above, we calculated a low value from their spectra that matches the low value reported by Pinkernell et al.²¹

11. Yang, X.; Ma, K. *Anal. Biochem.*, **2005**, *344*, 130–134.
12. van Hellemond, E. W.; Van Dijk, M.; Heuts, D. P.; Janssen, D. B.; Fraaije, M. W. *Appl. Microbiol. Biotechnol.*, **2008**, *78*, 455–463.
13. Liu, H.; Wang, Y.-S.; Wang, J.-C.; Xue, J.-H.; Zhou, B.; Zhao, H.; Liu, S.-D.; Tang, X.; Chen, S.-H.; Li, M.-H. *Anal. Biochem.*, **2014**, *458*, 4–10.
14. Tomari, N.; Sasamoto, K.; Sakai, H.; Tani, T.; Yamamoto, Y.; Nishiya, Y. *Anal. Biochem.*, **2019**, *584*, 113353.
15. Sugiyama, Y.; Ohta, H.; Hirano, R.; Shimokawa, H.; Sakana-ka, M.; Koyanagi, T.; Kurihara, S. *Anal. Biochem.*, **2020**, *593*, 113607.
16. Maruthamuthu, P.; Venkatasubramanian, L.; Dharmalingam, P. *Bull. Chem. Soc. Japan*, **1987**, *60*, 1113–1117.
17. Scott, S. L.; Chen, W. J.; Bakac, A.; Espenson, J. H. *J. Phys. Chem.*, **1993**, *97*, 6710–6714.
18. Lee, Y.; Yoon, J.; von Gunten, U. *Water Res.*, **2005**, *39*, 1946–1953.
19. Fan, W.; Qiao, J.; Guan, X. *Chemosphere*, **2017**, *171*, 460–467.
20. McBeath, S. T.; Wilkinson, D. P.; Graham, N. J. *Chemosphere*, **2020**, *251*, 126626.
21. Pinkernell, U.; Nowack, B.; Gallard, H.; Von Gunten, U. *Water Res.*, **2000**, *34*, 4343–4350.
22. Arnao, M. B.; Cano, A.; Hernandez-Ruiz, J.; Garcia-Cánovas, F.; Acosta, M. *Anal. Biochem.*, **1996**, *236*, 255–261.
23. Cano, A.; Acosta, M.; Arnao, M. B. *Redox Report*, **2000**, *5*, 365–370.
24. Re, R.; Pellegrini, N.; Proteggente, A.; Pannala, A.; Yang, M.; Rice-Evans, C. *Free Radical Biol. Med.*, **1999**, *26*, 1231–1237.
25. Noacco, N.; Rodenak-Kladniew, B.; de Bravo, M. G.; Castro, G. R.; Islan, G. A. *Anal. Biochem.*, **2018**, *555*, 59–66.
26. Zhang, W.; Jiang, H.; Yang, J.; Jin, M.; Du, Y.; Sun, Q.; Cao, L.; Xu, H. *Anal. Biochem.*, **2019**, *587*, 113460.
27. Ilyasov, I. R.; Beloborodov, V. L.; Selivanova, I. A.; Terekhov, R. P. *Int. J. Molec. Sci.*, **2020**, *21*, 1131.
28. Pichla, M.; Bartosz, G.; Pieńkowska, N.; Sadowska-Bartos, I. *Anal. Biochem.*, **2020**, *597*, 113698.
29. Hünig, S.; Balli, H.; Conrad, H.; Schott, A. *Justus Liebigs Annalen der Chemie*, **1964**, *676*, 52–65.

Appendix

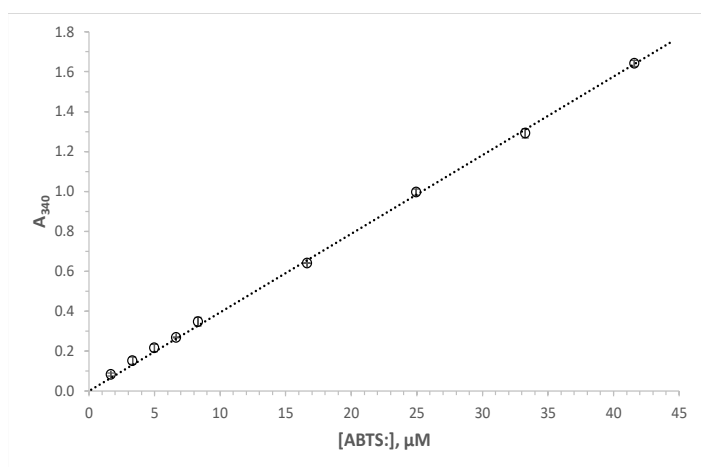


Figure S3. ABTS: calibration curve. Error bars (one standard deviation from triplicate measurements) are smaller than point symbols. Slope = $39.4 \pm 0.3 \text{ mM}^{-1}$; $R^2 = 0.9996$.

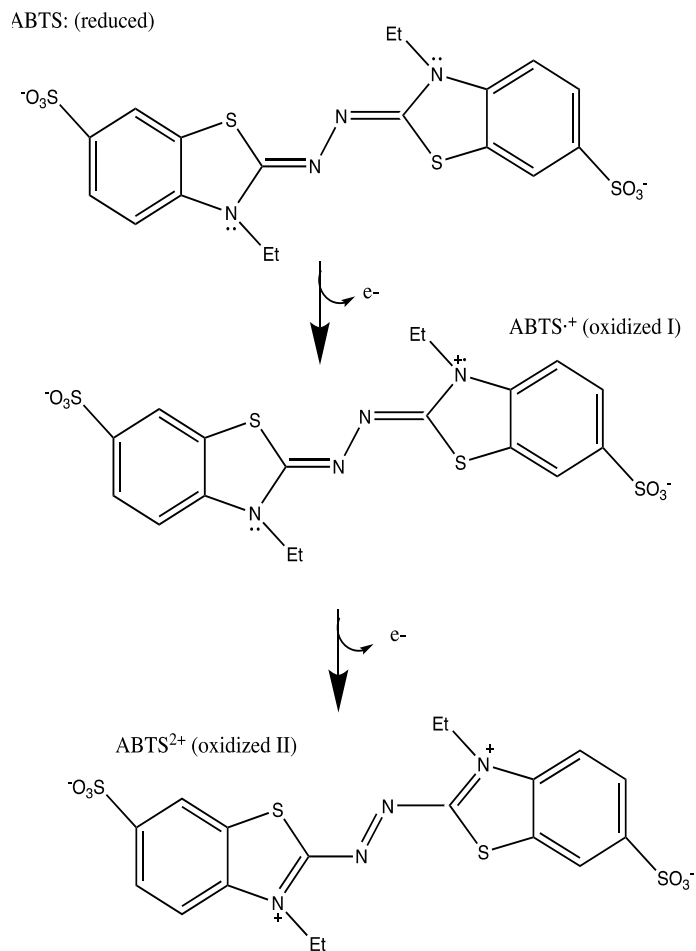


Figure S1. Oxidation of ABTS

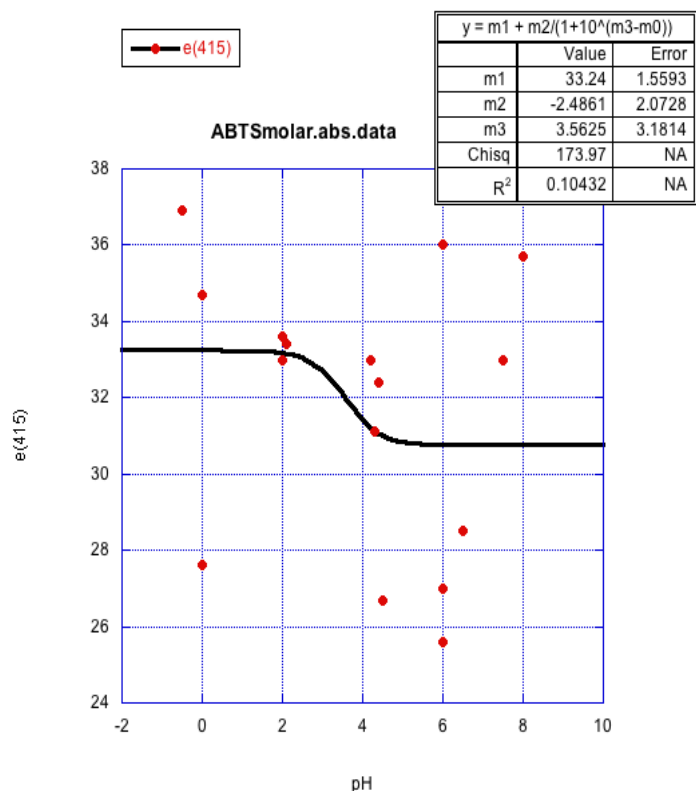


Figure S2. ABTS^{•+} molar absorptivity dependence on pH is statistically insignificant. Data from Table 1.

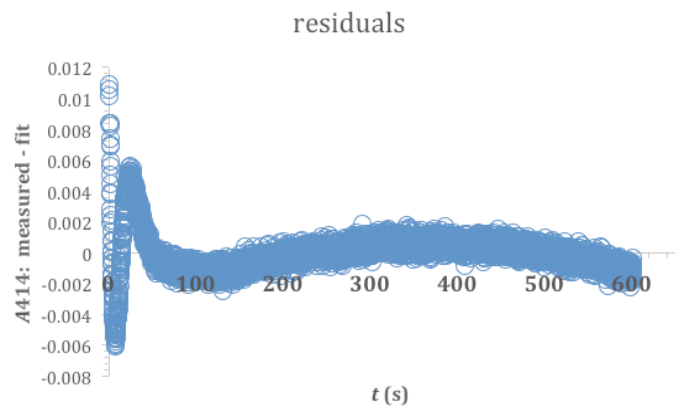


Figure S4: Residuals ($A_{414,obs} - A_{414,fit}$) for the data from Figure 2. Essentially all of the residuals (99.9%) lie between -0.006 and +0.006, which is less than the uncertainty in the absorbance measurement.